Published in final edited form as:
Science. 2010 October 1; 330(6000): 105–109. doi:10.1126/science.1191086.

The Calcium Store Sensor, STIM1, Reciprocally Controls Orai and $Ca_V1.2$ Channels

Youjun Wang[1], **Xiaoxiang Deng**[1,*], **Salvatore Mancarella**[1,*], **Eunan Hendron**[1,*], **Satoru Eguchi**[2], **Jonathan Soboloff**[1], **Xiang D. Tang**[3], and **Donald L. Gill**[1,†]

[1]Department of Biochemistry and Cardiovascular Research Center, Temple University School of Medicine, 3400 North Broad Street, Philadelphia, PA 19140, USA

[2]Department of Physiology, Temple University School of Medicine, Philadelphia, PA 19140, USA

[3]Department of Pharmacology, Nankai University School of Medicine, Tianjin 300071, China

Abstract

Calcium signals, pivotal in controlling cell function, can be generated by calcium entry channels activated by plasma membrane depolarization or depletion of internal calcium stores. We reveal a regulatory link between these two channel subtypes mediated by the ubiquitous calcium-sensing STIM proteins. STIM1 activation by store depletion or mutational modification strongly suppresses voltage-operated calcium ($Ca_V1.2$) channels while activating store-operated Orai channels. Both actions are mediated by the short STIM-Orai activating region (SOAR) of STIM1. STIM1 interacts with $Ca_V1.2$ channels and localizes within discrete endoplasmic reticulum/plasma membrane junctions containing both $Ca_V1.2$ and Orai1 channels. Hence, STIM1 interacts with and reciprocally controls two major calcium channels hitherto thought to operate independently. Such coordinated control of the widely expressed $Ca_V1.2$ and Orai channels has major implications for Ca^{2+} signal generation in excitable and nonexcitable cells.

Ca^{2+} entry channels, crucial in providing cellular Ca^{2+} signals, are controlled by sensing mechanisms, including membrane voltage, surface receptors, and Ca^{2+}-sensing STIM proteins in the endoplasmic reticulum (ER) (1). The coordinated operation of these transduction processes is key to controlling cell function. STIM proteins are dynamic ER Ca^{2+} sensors that aggregate when ER is depleted of Ca, then rapidly translocate into ER-plasma membrane (PM) junctions, where they interact with and activate the highly Ca^{2+}-selective Orai family of PM channels (2, 3). We determined that STIM proteins also mediate inhibitory control of voltage-activated $Ca_V1.2$ channels. This action was independent of Orai channel function or changes in cytosolic Ca^{2+} and was mediated by a direct action of STIM1 on the $Ca_V1.2$ α_{1C} subunit. Thus, STIM1 reciprocally controls Orai and $Ca_V1.2$ channels, indicating a hitherto unknown and potentially crucial regulatory link between receptor-induced Ca^{2+} store depletion and control of voltage-activated Ca^{2+} signals.

We studied STIM1-mediated Ca^{2+} entry signals in A7r5 clonal vascular smooth muscle cells (VSMC). Ca^{2+} store depletion by vasopressin (VP) or ER Ca^{2+} pump blockade by

†To whom correspondence should be addressed: dgill@temple.edu.
*These authors contributed equally to this work.

Supporting Online Material
www.sciencemag.org/cgi/content/full/330/6000/105/DC1
Materials and Methods
Figs. S1 to S4
Table S1
References

thapsigargin (TG) induced a large Ca^{2+} influx across the PM when Ca^{2+} was added externally (Fig. 1, A and B). However, the inwardly rectifying Ca^{2+}-release activated Ca^{2+} (CRAC) current mediating this Ca^{2+} entry was barely measurable (Fig. 1B, inset) because only a small number of Ca^{2+} ions flow through these highly selective channels. Expression in A7r5 cells of the STIM1-D76A mutant defective in sensing ER Ca^{2+} (1) selectively activated Ca^{2+} entry (almost no entry of Sr^{2+}) (Fig. 1C), which required no store emptying. Expression of the E106A Orai1 mutant lacking a functional pore and acting as a dominant negative on Orai channels (4, 5) completely eliminated VP- or TG-induced Ca^{2+} entry (Fig. 1A and B), revealing that entry is exclusively Orai-mediated.

Canonical transient receptor potential (TRPC) channels, widely reported to contribute to store-induced Ca^{2+} entry (1, 6), are highly expressed in VSMCs (7). In A7r5 cells, a large nonselective current activated by VP and mediated by TRPCs (7) was not influenced by store depletion or by expression of the dominant Orai1-E106A mutant or the constitutively active STIM1-D76A mutant, reinforcing recent evidence (8) against a role of STIM proteins or Ca^{2+} stores in TRPC channel function. In contrast, endogenous $Ca_V1.2$ channels did respond to emptying of intracellular Ca^{2+} stores. In A7r5 cells, Sr^{2+} entry through $Ca_V1.2$ channels was activated by a depolarizing pulse of high extracellular [K^+] and blocked by the $Ca_V1.2$-specific blocker nimodipine (Fig. 1D). If 2 μM ionomycin or 2 μM TG was added to deplete Ca^{2+} stores, a subsequent depolarizing pulse resulted in greatly decreased $Ca_V1.2$-mediated entry of Sr^{2+} (Fig. 1, E and G). However, although VP treatment also induced Ca^{2+} store depletion, $Ca_V1.2$-mediated Sr^{2+} entry was instead enhanced (Fig. 1, F and G), likely due to activation of $Ca_V1.2$ channels by Ca^{2+}- and diacylglcycerol-induced protein kinase C stimulation (9, 10). To more directly examine the actions of store emptying on $Ca_V1.2$ channels, we measured $Ca_V1.2$ currents by patch-clamping cells with cytosolic Ca^{2+} buffered at physiological resting levels with the Ca^{2+} chelator EGTA to prevent any Ca^{2+}-dependent changes in $Ca_V1.2$ function. Compared with control $Ca_V1.2$ peak current (0.28 ± 0.08 pA/pF), store depletion by ionomycin inhibited $Ca_V1.2$ current by 96% (0.01 ± 0.02 pA/pF; $n = 6$, $P = 0.001$) (Fig. 1H). Store depletion with VP also reduced current by 58% (0.11 ± 0.06 pA/pF; $n = 6$, $P = 0.004$). Thus, Ca^{2+} buffering revealed a consistent store depletion–mediated inhibition of $Ca_V1.2$ channels. We further examined the influence of Ca^{2+} store depletion on $Ca_V1.2$ channels expressed in human embryonic kidney (HEK293) cells. Nimodipine-sensitive, depolarization-induced Sr^{2+} entry (Fig. 1I) with typical $Ca_V1.2$ current-voltage relationship (inset) was observed in HEK293 cells expressing the three $Ca_V1.2$ component subunits α_{1C}, β_{2a}, and $\alpha_2\delta_1$. Ca^{2+} store depletion with ionomycin or ER Ca^{2+} pump blocker di-tertbutylhydroquinone (DBHQ) substantially reduced $Ca_V1.2$-mediated Sr^{2+} entry compared with control cells (Fig. 1, J and K). Application of the cell-permeant intraluminal ER-Ca^{2+} chelator, *N*, *N*,*N*′,*N*′-tetrakis(2-pyridylmethyl)-ethylenediamine (TPEN), caused a similar decrease (Fig. 1K). TPEN reduces ER-Ca^{2+} with no increase in cytosolic Ca^{2+} (11), confirming that store depletion inhibits $Ca_V1.2$ channels independent of cytosolic Ca^{2+} changes.

The ER Ca^{2+} sensors, STIM1 and STIM2, are triggered by ER Ca^{2+} depletion to translocate and activate PM Orai channels (1). We investigated the role of STIM proteins in store depletion–induced inhibition of $Ca_V1.2$ channels. Using $Ca_V1.2$ ($\alpha_{1C} + \beta_{2a} + \alpha_2\delta_1$)–transfected HEK293 cells, overexpressed yellow fluorescent protein–fusion constructs (YFP-STIM1 or YFP-STIM2) (fig. S1, A to D) had little effect on $Ca_V1.2$-mediated Sr^{2+} entry in store-replete cells (Fig. 2A). However, YFP-STIM1 expression greatly increased the inhibitory effect of ionomycin-induced store depletion on $Ca_V1.2$-mediated Sr^{2+} entry (Fig. 2A). Similar expression of YFP-STIM2 had a smaller effect. STIM2 is similarly poorer in coupling to activate Orai channels (1, 12, 13). Although native STIM1 is expressed in both ER and PM, YFP-STIM1 is exclusively expressed in ER (1, 14); thus, the action of STIM1 on $Ca_V1.2$ function is mediated by ER-STIM1.

We examined how STIM1 and Orai1 RNA interference (RNAi) influenced endogenous $Ca_V1.2$ channels in A7r5 cells. STIM1-siRNA (small interfering RNA) increased $Ca_V1.2$-mediated Sr^{2+} entry in store-replete cells (Fig. 2B), suggesting that some endogenous STIM1 exists in junctions and constitutively inhibits $Ca_V1.2$. Orai1-siRNA had little effect. STIM1-siRNA had little effect on store depletion–induced inhibition of $Ca_V1.2$ channels (Fig. 2C). However, although RNAi reduced STIM1 expression by ~80% (fig. S2A), store emptying may efficiently cause the remaining 20% to enter ER-PM junctions, perhaps explaining the differential effectiveness of STIM1-RNAi on $Ca_V1.2$ activity in store-replete versus store-depleted cells. A combination of STIM1- and Orai1-siRNA resulted in a substantial reduction in the inhibition of $Ca_V1.2$ channels by store depletion (Fig. 2C). After store depletion, Orai1 traps STIM1 within ER-PM junctions (15); thus, with limited STIM1 in RNAi-treated cells, endogenous Orai1 may be necessary to bring STIM1 to the PM where it can alter $Ca_V1.2$ channels.

STIM1 EF-hand mutants fail to bind Ca^{2+} (16–18), aggregate and translocate into ER-PM junctions, and constitutively activate Orai1 channels without requiring changes in ER Ca^{2+} (18). Expression of YFP-STIM1-D76A EF-hand mutant in A7r5 cells led to a constitutive reduction in the function of endogenous $Ca_V1.2$ channels (Fig. 2D). Cells with visible YFP expression had >70% reduced $Ca_V1.2$-mediated Sr^{2+} entry, and almost all mutant STIM1 was within clearly discernible junctions (fig. S2B). There was little difference in resting cytosolic [Ca^{2+}] in D76A-expressing cells (fig. S2C), consistent with studies on cells stably expressing D76A (19). Cells with no detectable fluorescence had 40% reduced $Ca_V1.2$ function (Fig. 2D) and no change in resting Ca^{2+} (fig. S2C). Hence, the action of STIM1 on $Ca_V1.2$ channel function is independent of both luminal and cytosolic Ca^{2+} changes.

The same inhibitory effect of STIM1-D76A was observed on Sr^{2+} entry through $Ca_V1.2$ channels expressed in HEK cells (Fig. 2E). Coexpression of the dominant negative Orai1-E106A mutant did not alter the STIM1-D76A–induced inhibition of $Ca_V1.2$ channels, although it completely blocked the constitutive Ca^{2+} entry observed after addition of Ca^{2+} in STIM1-D76A–expressing cells after washout of the K^+/Sr^{2+} solution (Fig. 2E, red versus green traces). Hence, we conclude that the inhibitory effect of STIM1 on $Ca_V1.2$ channels does not require Orai channel function and does not reflect any passage of ions through store-operated channels.

$Ca_V1.2$ channels comprise three subunits: the α_{1C} pore-forming moiety and the β and $\alpha_2\delta_1$ auxiliary subunits (10). STIM1-mediated $Ca_V1.2$ inhibition did not require the auxiliary proteins. As for HEK293 cells expressing all three $Ca_V1.2$ subunits, cells expressing only the α_{1C} subunit had depolarization-induced Sr^{2+} entry inhibited by TPEN (Fig. 2F), enhanced with STIM1 or STIM2 overexpression (fig. S3, A to C) and mimicked by STIM1-D76A expression independently of Orai function (Fig. 2G). STIM1-D76A did not alter α_{1C} expression or vice versa, and α_{1C} did not alter STIM1-D76A localization (fig. S3, D and E).

To address whether $Ca_V1.2$ α_{1C} interacts with STIM1, we undertook coimmunoprecipitation studies using green fluorescent protein (GFP)–tagged α_{1C} and either native or mCherry-tagged STIM1. Coexpressed in HEK cells, antibody to STIM1 precipitates contained GFP-α_{1C} (Fig. 3A). Moreover, precipitates of GFP-α_{1C} with antibody to GFP revealed bound STIM1 (Fig. 3B). Although interactions between the two proteins exist, store depletion did not detectably alter this association. We undertook high-resolution imaging studies to examine distribution of STIM1, $Ca_V1.2$ channels, and Orai channels at the PM (19). We expressed N-tagged GFP-α_{1C} (20), β_{2a} and $\alpha_2\delta_1$ subunits, and N-tagged mCherry-STIM1 (19). High-resolution imaging of the ER-PM junctions adjacent to the coverslip revealed precise colocalization between mCherry-STIM1 and GFP-α_{1C} induced by emptying Ca^{2+} stores with ionomycin (Fig. 3, C to K). Ionomycin-mediated store

depletion for 5 min induced mCherry-STIM1 to move into clearly defined ER-PM junctional areas (Fig. 3, C and F). GFP-$Ca_V1.2$ moved into the same areas (Fig. 3, D, G, and H). High magnification of the boxed areas (Fig. 3, I to K) reveals the precise nature of the colocalization of the two proteins after store depletion. There were no areas of STIM1 not colocalized with α_{1C}, although there were areas of α_{1C} extending beyond the STIM1-defined junctional areas. Small areas with colocalized STIM-$Ca_V1.2$ were evident in store-replete cells (Fig. 3, C to E). This indicates a possible constitutive role of STIM1 in attenuating $Ca_V1.2$ activity, consistent with the effect of STIM1 RNAi on $Ca_V1.2$ function (Fig. 2B). We also coexpressed mCherry-Orai1 [exclusively PM-localized (18)] with GFP-α_{1C} in stable STIM1-expressing HEK cells, revealing areas of Orai1-$Ca_V1.2$ colocalization after store depletion (Fig. 3, L to O). Such Orai1-localization is exclusively STIM-associated (1, 18); hence, ER-PM junctions appear to contain a complex of Orai1, $Ca_V1.2$, and STIM proteins.

We investigated whether STIM1 domains coupling to Orai were also coupling to α_{1C} and whether Orai might participate in STIM-α_{1C} coupling. The smallest units of STIM1 to bind and activate Orai1 are the 344-442 STIM-Orai activating region (SOAR) (21) and 342-448 Ca^{2+}-activating domain (CAD) (15) (Fig. 4A). We transfected YFP-SOAR into HEK293 cells expressing α_{1C} (Fig. 4, B to F). $Ca_V1.2$ channels were activated with K^+/Sr^{2+}, then blocked with nimodipine, followed by Ca^{2+} addition to observe Orai function. In non-SOAR–expressing cells, there was full α_{1C} channel activity and no Orai function (Fig. 4B). In cells cotransfected with SOAR (Fig. 4C), a clear correlation existed between Orai activation, α_{1C} inhibition, and SOAR expression (Fig. 4, C and D, and fig. S4A). Cells with full α_{1C}-mediated Sr^{2+} entry had no Orai-induced Ca^{2+} entry (green), whereas cells with a large reduction in α_{1C} function showed Orai-induced Ca^{2+} entry (blue). The Orai-coupled cells had ~50% greater SOAR levels (fig. S4B); thus, SOAR coupling to both α_{1C} and Orai exactly correlated. Coexpressing Orai1-E106A with α_{1C} and SOAR (Fig. 4D) caused SOAR to be more consistently PM-associated (Fig. 4E), and α_{1C} channel activity was inhibited in all cells (Fig. 4D and fig. S4A). Thus, Orai may assist SOAR associating with the PM and inhibit α_{1C}; however, the Orai channel need not be functional to pull SOAR toward α_{1C} and inhibit α_{1C} function. Expression of the LQ347/348AA SOAR mutant (Fig. 4F) devoid of coupling to Orai1 (21) did not inhibit α_{1C} function, with or without Orai1-E106A (Fig. 4G), and did not associate with Orai1 at the PM (Fig. 4H). We expressed the STIM1 C terminus (YFP-STIM1-CT; 235-685) (Fig. 4, F, I, and J), which is largely cytosolic (15, 18). Coexpressed with Orai channels, some STIM1-CTassociates with Orai1 (Fig. 4J). STIM1-CT expressed with α_{1C} caused no change in $Ca_V1.2$ activity consistent with its cytosolic location (18). However, coexpressed with Orai1-E106A, the STIM1-CT gave substantial reduction in α_{1C} activity (Fig. 4I), indicating that the association between STIM1-CT and Orai1 was sufficient for STIM1-CT to inhibit α_{1C}.

The far C-terminal K-rich region of STIM1, although not essential for Orai1 activation, assists STIM1-induced association with PM junctions (15). Compared with wild-type STIM1, STIM1ΔK (Δ667-685) (Fig. 4, A and F) was less effective in inhibiting α_{1C} function after store depletion (Fig. 4K and fig. S4C), indicating that the K-rich region enhances PM docking of STIM1 and association with α_{1C}. The STIM1Δ441-448 deletion (Fig. 4A) does not activate Orai1 channels and does not block endogenous STIM1-mediated Ca^{2+} influx (Fig. 4L) and is likely defective in Orai1-binding. However, STIM1Δ441-448 does still inhibit α_{1C}-mediated Sr^{2+} entry almost identical to wild-type STIM1 (Fig. 4K and fig. S4C). Thus, the site on STIM1 coupling to inhibit $Ca_V1.2$ channels is not identical to that mediating Orai channel activation. Moreover, the action of STIM1 on $Ca_V1.2$ channels does not require Orai channel activation, despite Orai channels assisting STIM1's approach to $Ca_V1.2$ channels.

The work herein provides evidence that the $Ca_V1.2$ channel is an authentic target of STIM proteins, in addition to their well-described Orai targets. The reciprocal control mediated by STIM on the Orai and $Ca_V1.2$ channel targets may have functional implications in many cells expressing both channels. Although we reveal that the action of STIM1 on $Ca_V1.2$ channels does not require the function of Orai channels, we do reveal that the actions of STIM1 on Orai1 and $Ca_V1.2$ channels are closely connected, both spatially and functionally. Orai channels are very effective at trapping STIM1 in puncta (15) and appear to enhance STIM1 recruitment to the vicinity of $Ca_V1.2$ channels in the PM. $Ca_V1.2$ proteins are widely expressed not only in excitable cells but also nonexcitable cells—for example, immune cells including T cells, B cells, dendritic cells, and mast cells (22, 23). STIM proteins may have important roles in suppressing $Ca_V1.2$ function in immune cells, and STIM-mediated reciprocal control of $Ca_V1.2$ and Orai channels could be a decisive mechanism for controlling Ca^{2+} signals. STIM proteins are highly expressed in many excitable tissues, including smooth muscle cells (24, 25), neurons (26), and skeletal muscle (27), where they have been implicated in mediating not only Ca^{2+} signals but also fundamental control over growth, differentiation, and apoptosis (25–27). The finding of reciprocal control of the two major and widely expressed Ca^{2+} channels by a single Ca^{2+}-sensing regulatory protein should enhance understanding of Ca^{2+} signal transduction.

Supplementary Material

Refer to Web version on PubMed Central for supplementary material.

Acknowledgments

Rabbit smooth muscle α_{1C}, β_{2a}, and α_2-δ_1 DNA were gifts from M. Davis, University of Missouri School of Medicine. This work was supported by NIH grants HL55426 and AI058173 (D.L.G.), a Novartis Institutes for Biomedical Research fellowship (Y.W.), the American Heart Association (J.S.), NSFC 30871011, Tianjin S&T Support Project 08ZCKFSH04500, and “973” program 2010CB945001 (X.P.T.).

References and Notes

1. Deng X, Wang Y, Zhou Y, Soboloff J, Gill DL. J Biol Chem. 2009; 284:22501. [PubMed: 19473984]
2. Lewis RS. Nature. 2007; 446:284. [PubMed: 17361175]
3. Cahalan MD. Nat Cell Biol. 2009; 11:669. [PubMed: 19488056]
4. Soboloff J, et al. J Biol Chem. 2006; 281:20661. [PubMed: 16766533]
5. Lis A, et al. Curr Biol. 2007; 17:794. [PubMed: 17442569]
6. Yuan JP, et al. Channels (Austin). 2009; 3:221. [PubMed: 19574740]
7. Soboloff J, et al. J Biol Chem. 2005; 280:39786. [PubMed: 16204251]
8. DeHaven WI, et al. J Physiol. 2009; 587:2275. [PubMed: 19332491]
9. Shistik E, Ivanina T, Blumenstein Y, Dascal N. J Biol Chem. 1998; 273:17901. [PubMed: 9651396]
10. Dai S, Hall DD, Hell JW. Physiol Rev. 2009; 89:411. [PubMed: 19342611]
11. Hofer AM, Fasolato C, Pozzan T. J Cell Biol. 1998; 140:325. [PubMed: 9442108]
12. Soboloff J, et al. Curr Biol. 2006; 16:1465. [PubMed: 16860747]
13. Zhou Y, et al. J Biol Chem. 2009; 284:19164. [PubMed: 19487696]
14. Baba Y, et al. Proc Natl Acad Sci USA. 2006; 103:16704. [PubMed: 17075073]
15. Park CY, et al. Cell. 2009; 136:876. [PubMed: 19249086]
16. Liou J, et al. Curr Biol. 2005; 15:1235. [PubMed: 16005298]
17. Spassova MA, et al. Proc Natl Acad Sci USA. 2006; 103:4040. [PubMed: 16537481]
18. Wang Y, et al. Proc Natl Acad Sci USA. 2009; 106:7391. [PubMed: 19376967]
19. Hewavitharana T, et al. J Biol Chem. 2008; 283:26252. [PubMed: 18635545]

20. Grabner M, Dirksen RT, Beam KG. Proc Natl Acad Sci USA. 1998; 95:1903. [PubMed: 9465115]
21. Yuan JP, et al. Nat Cell Biol. 2009; 11:337. [PubMed: 19182790]
22. Matza D, Flavell RA. Immunol Rev. 2009; 231:257. [PubMed: 19754902]
23. Suzuki Y, Inoue T, Ra C. Mol Immunol. 2010; 47:640. [PubMed: 19926136]
24. Wang Y, Deng X, Hewavitharana T, Soboloff J, Gill DL. Clin Exp Pharmacol Physiol. 2008; 35:1127. [PubMed: 18782202]
25. Potier M, et al. FASEB J. 2009; 23:2425. [PubMed: 19364762]
26. Berna-Erro A, et al. Sci Signal. 2009; 2:ra67. [PubMed: 19843959]
27. Stiber J, et al. Nat Cell Biol. 2008; 10:688. [PubMed: 18488020]

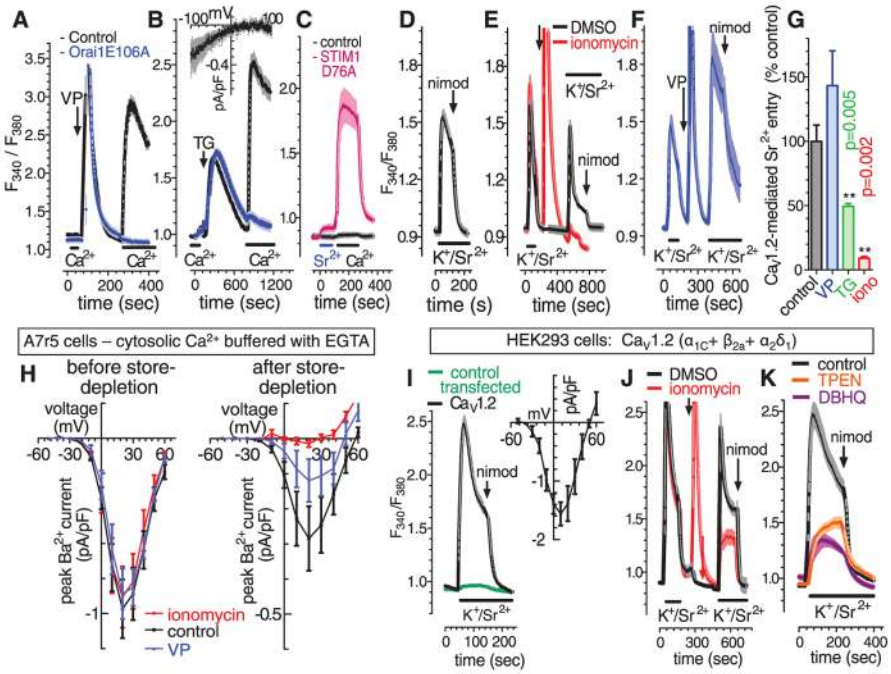

Fig. 1.

Store-dependent control of Orai and $Ca_V1.2$ channels. Fura-2 F_{340}/F_{380} ratiometric responses to cytosolic Ca^{2+} in A7r5 VSMCs in response to 100 nM VP (**A**) or 2 μM TG (**B**), in control or Orai1-E106A-CFP–transfected cells in nominally Ca^{2+} free or 3 mM external Ca^{2+} (bars). (Inset) Current-voltage curve for CRAC channels in control A7r5 cells. (**C**) Fura-2 responses in control and STIM1-D76A–transfected A7r5 cells (bars, 3 mM external Sr^{2+} or Ca^{2+}). (**D**) Fura-2 responses to application of external 134 mM K^+ with 3 mM Sr^{2+} (bars, K^+/Sr^{2+}); 2 μM nimodipine (arrow). (**E**) Fura-2 responses to two sequential K^+/Sr^{2+} pulses (bars) with addition of dimethyl sulfoxide (DMSO) or 2 μM ionomycin (arrow), and subsequent 2 μM nimodipine addition. (**F**) As in (E), except with the addition of 100 nM VP. (**G**) Statistics for results in (E), (F), and TG (trace not shown) ($n = 6$, paired t test). (**H**) I/V curve for whole-cell Ba^{2+} current through $Ca_V1.2$ channels in A7r5 cells with cytosolic Ca2+ clamped to 0.1 μM (10 mM EGTA; 3.4 mM $CaCl_2$), either before (left) or 5 min after store depletion with 2 μM ionomycin, 100 nM VP, or control (right). **(I** to **K)** Fura-2 responses to K^+/Sr^{2+} (bars) in HEK293 cells expressing three $Ca_V1.2$ subunits (α_{1C}+ β_{2a}+ $\alpha_2\delta_1$) or control-transfected cells. (I) K^+/Sr^{2+} responses in $Ca_V1.2$-transfected and control-transfected cells; 2 μM nimodipine (arrow); inset, I/V curve for $Ca_V1.2$-transfected cells (n = 4). (J) Fura-2 responses to sequential K^+/Sr^{2+} pulses (bars) with additions of DMSO or 2 μM ionomycin (arrow), and 2 μM nimodipine (arrows). (K) K^+/Sr^2 responses after DBHQ (10 μM, 10 min, present throughout) or TPEN (250 μM, 5 min, removed at K^+/Sr^{2+} addition).

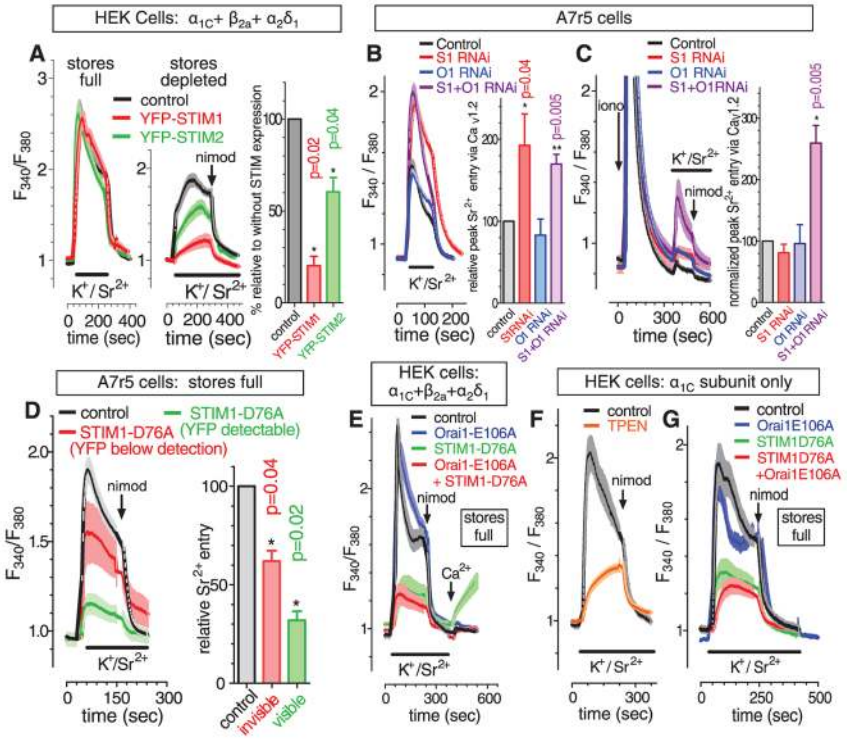

Fig. 2.

STIM proteins mediate store depletion–induced control of $Ca_V1.2$ channels. (**A**) HEK293 cells expressing α_{1C} + β_{2a}+ $\alpha_2\delta_1$ $Ca_V1.2$ channel subunits; fura-2 responses to K^+/Sr^{2+} pulses (bars) before (left) and after (middle) store emptying with 2 μM ionomycin and subsequent 2 μM nimodipine addition (arrow). Statistics (right), paired *t* test, $n = 6$. (**B**) Store-replete A7r5 cells treated either with STIM1 RNAi, Orai1 RNAi, STIM1+Orai1 RNAi, or control RNAi; left, fura-2 responses to K^+/Sr^{2+} pulse (bar); right, statistics (paired *t* test, $n = 8$). (**C**) The same RNAi-treated cells used in (B) were then store-depleted with 2 μM ionomycin (arrow); left, fura-2 responses to K^+/Sr^{2+} pulse (bar); right, statistics (paired *t* test, $n = 8$). (**D**) Store-replete A7r5 cells either control-transfected or transfected with YFP-STIM1-D76A (cells with detectable or undetectable YPP on a single coverslip); left, fura-2 responses to K^+/Sr^{2+} pulse (bar) and 2 μM nimodipine (arrow); right, statistics (paired *t* test, $n = 8$). (**E**) HEK293 cells expressing α_{1C} + β_{2a}+ $\alpha_2\delta_1$ $Ca_V1.2$ channel subunits cotransfected with either Orai1-E106A-CFP, YFP-STIM1-D76A, Orai1-E106A-CFP + YFP-STIM1-D76A, or control plasmid; fura-2 responses to K^+/Sr^{2+} pulse (bar), 2 μM nimodipine (arrow) and 3 mM Ca^{2+} (arrow). (**F**) HEK293 cells expressing α_{1C} alone; fura-2 response to K^+/Sr^2 pulse (bar) and 2 μM nimodipine (arrow) in cells either TPEN-treated (250 μM, 5 min, removed at K^+/Sr^{2+} addition) or untreated. (**G**) HEK293 cells expressing α_{1C} cotransfected with either Orai1-E106A-CFP, YFP-STIM1-D76A, Orai1-E106A-CFP + YFP-STIM1-D76A, or control plasmid; fura-2 response to K^+/Sr^{2+} pulse (bar), and 2 μM nimodipine (arrow).

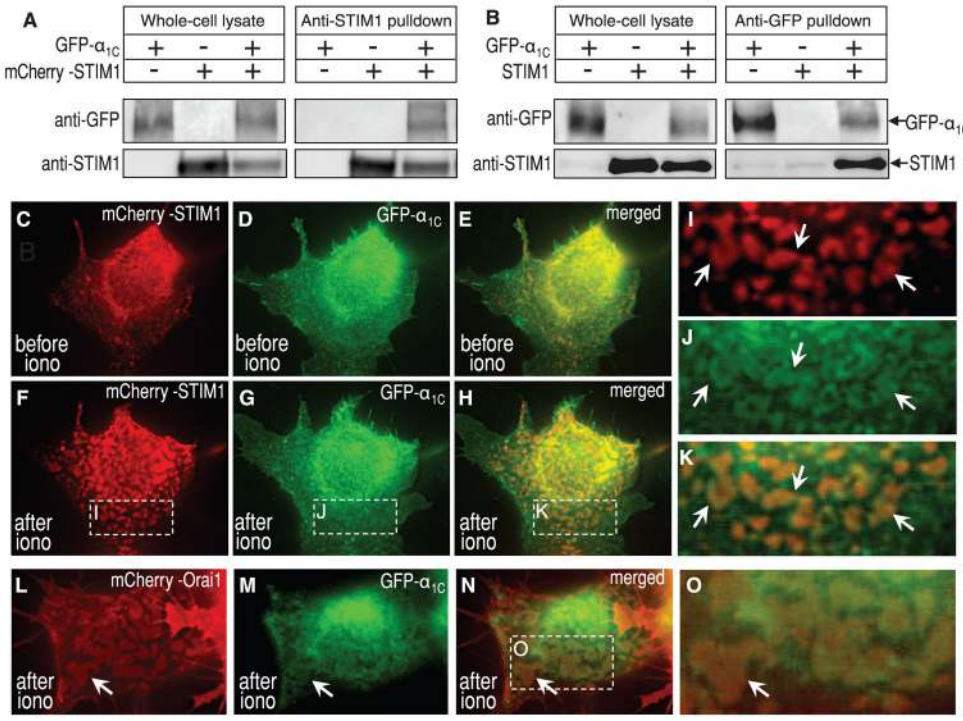

Fig. 3.

Interactions between STIM1 and $Ca_V1.2$ α_{1C}, and store-dependent co-localization of STIM1, $Ca_V1.2$, and Orai1 proteins. (**A**) HEK293 cells coexpressing mCherry-STIM1 and GFP-α_{1C}; whole-cell lysates (left) and antibody to STIM1 immunoprecipitates were probed with antibody to GFP and antibody to STIM1. (**B**) HEK293 cells coexpressing GFP-α_{1C} and STIM1; whole-cell lysates (left) and antibody to GFP immunoprecipitates were probed with antibody to GFP and antibody to STIM1. (**C** to **O**) High-resolution imaging focused on the ER-PM interface in HEK293 cells. (C to H) Distribution of expressed mCherry-STIM1 and GFP-α_{1C} (coexpressed with β_{2a} + $\alpha_2\delta_1$ subunits), examined in cells either just before (C and E) or 5 min after (F to H) Ca^{2+} store depletion with 2 μM ionomycin. (**I** to **K**) Magnification of the STIM, α_{1C}, and merged images, respectively. (L and M) Distribution of coexpressed mCherry-Orai1 and GFP-α_{1C} (with β_{2a} + $\alpha_2\delta_1$ subunits) in cells 5 min after ionomycin-induced emptying. (**O**) Magnified area of the merged image from (N).

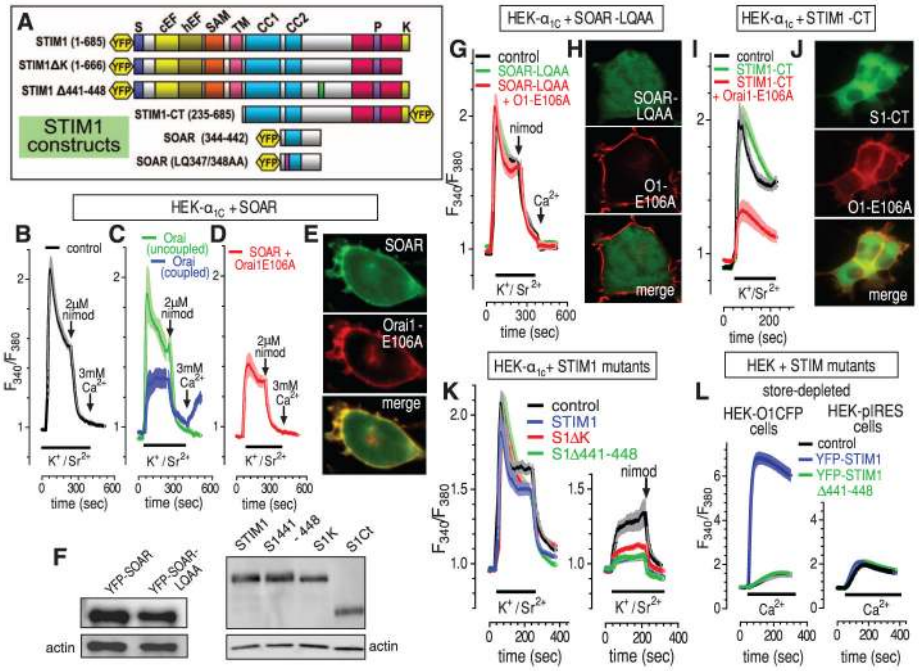

Fig. 4.

Defining the molecular domains of STIM1 mediating $Ca_V1.2$ channel inhibition. (**A**) STIM1 constructs used. (**B** to **D**) Fura-2 responses to K^+/Sr^{2+} pulses (bars), 2 μM nimodipine, and 3 mM Ca^{2+} (arrows) in α_{1C}-expressing HEK293 cells without cotransfection (B) or with cotransfection of YFP-SOAR (C) or YFP-SOAR + Orai1-E106A-CFP (D). Statistics shown in fig. S4A. In (C), Orai-coupled ($n = 97$; cells with Orai-mediated Ca^{2+} entry) and Orai-uncoupled ($n = 135$; cells with no Orai-mediated Ca^{2+} entry) are defined in the text. Their relative YFP-SOAR expression is shown in fig. S4B. (**E**) Localization of YFP-SOAR + Orai1-E106A-CFP cotransfected cells. (**F**) Western analysis of STIM construct expression. (**G**) Fura-2 responses in α_{1C}-expressing HEK293 cells cotransfected with YFP-SOAR-LQ347/348AA alone or with Orai-E106A-CFP. (**H**) Imaging of the mutant SOAR + Orai–expressing cells in (G). (**I**) Fura-2 responses in α_{1C}-expressing HEK293 cells cotransfected with YFP-STIM1-CT alone or with Orai-E106A-CFP. (**J**) Imaging of the STIM-CT + Orai–expressing cells in (I). (**K**) Fura-2 responses in α_{1C}-expressing HEK293 cells before (left) and after (right) store depletion with 2 μM ionomycin; cells were cotransfected with either normal STIM1, the STIM1-ΔK truncation (Δ667-685), the STIM1-Δ441-448 deletion, or empty plasmid (statistics shown in fig. S4C). (**L**) Fura-2 responses to 1 mM Ca^{2+} addition for Orai1-CFP–expressing HEK293 cells (left) or control internal ribosomal entry site plasmid (pIRES)–HEK cells (right) transfected with YFP-STIM1-wild-type or YFP-STIM1-Δ441-448.